Journal of Thermal Analysis and Calorimetry, Vol. 82 (2005) 783–789

CONSTANT TRANSFORMATION RATE THERMAL ANALYSIS OF $HGdP_2O_7{\cdot}3H_2O$

F. Chehimi-Moumen[1]*, P. Llewellyn*[2]*, F. Rouquerol*[2*]*, G. Vacquier*[2†]*,*
D. Ben Hassen–Chehimi[1]*, M. Ferid*[3] *and M. Trabelsi-Ayadi*[1]

[1]Laboratoire de Physico-Chimie Minérale, Faculté des Sciences de Bizerte,
7021 Zarzouna-Bizerte, Tunisia
[2]Laboratoire des Matériaux Divisés, Revêtements, Electrocéramiques, UMR 6121 Université de Provence–CNRS, Centre de Saint Jérôme, 13397 Marseille Cedex 20, France
[3]Laboratoire des Procédés Chimiques, Institut National de Recherche Scientifique et Technique. B.P. 95, Hammam-Lif, 2050, Tunisia

The aim of this work is the optimization of the preparation of anhydrous gadolinium hydrogen phosphate with good fluorescence properties. The products obtained by dehydration of gadolinium hydrogen phosphate trihydrate depend on the conditions chosen for the thermal treatment. For this reason, the dehydration was followed by Constant Rate Thermal Analysis whilst strictly controlling the water vapour pressure above the sample. Intermediate samples, obtained during dehydration were characterised by IR spectroscopy and X-ray diffraction. It has thus been shown that the thermal pathway taken for the dehydration depends on the water vapour pressure above the sample in the region from 10^{-2} to 5 mbar. Under the lowest water vapour pressure ($5{\cdot}10^{-3}$ mbar), the elimination of the crystallization water is carried out in a continuous way and produces a quasi-amorphous intermediate. Under higher water vapour pressure (5 mbar), well crystallized intermediate products are obtained. The results obtained suggest that the trihydrate contains zeolitic water which confirms a prior structural study.

Keywords: *gadolinium hydrogen phosphate trihydrate, sample controlled thermal analysis*

Introduction

The good fluorescence properties of the rare earth phosphate materials are well known. In particular $M^{I}Ln(PO_3)_4$ type polyphosphates and LnP_5O_{14} type ultraphosphates have been studied for high power laser application [1–7]. The fluorescence properties of other types of phosphate materials, such as the $M^{I}LnP_2O_7$ diphosphates or pyrophosphates (where M^{I}=Rb, Cs and *Ln*=Y, Dy, Gd), have been investigated during the last 20 years [8–9]. These phosphates are found to show very weak concentration quenching.

Studies concerning the protonated lanthanide diphosphates of general formula $HLnP_2O_7{\cdot}xH_2O$ show that these compounds can adopt at least three crystalline structures [10–13]. The first structural type concerns the $HLnP_2O_7{\cdot}3H_2O$ (*Ln*=La–Sm) compounds crystallizing in the Aba2 space group [14]. The second type concerns the $HLnP_2O_7{\cdot}3H_2O$ (*Ln*=Sm–Lu) which crystallizes in the P-1 space group [15]. The tetrahydrated samarium diphosphate $HSmP_2O_7{\cdot}4H_2O$ is another unique isolated compound with a third crystalline structure which crystallizes in the $P2_1/n$ space group [13].

In previous papers we have reported the crystal structure of the trihydrated acid gadolinium diphosphate crystallising in the first structural group [15] as well as its thermal behaviour studied by conventional thermogravimetry [16].

The thermogravimetric analysis of $HGdP_2O_7{\cdot}3H_2O$ carried out in an argon atmosphere with a 5 K min^{-1} heating rate shows that the three crystallization water molecules are removed in three stages between 344 and 773 K [16]. Intermediates obtained at 418 and 553 K with chemical compositions of $HGdP_2O_7{\cdot}1.5H_2O$ and $HGdP_2O_7{\cdot}0.5H_2O$ were obtained and the salt obtained at 773 K was identified as $HGdP_2O_7$.

It is widely accepted that conventional thermo gravimetry which subjects samples to a linear heating rate can have a major influence on the information content of the TG curve and on the properties of the heat treated products. This can be a source of irreproducibility and highlights the importance that Constant transformation Rate Thermal Analysis (CRTA) can have [17, 18]. CRTA permits a constant reaction rate slow enough to minimise the temperature and pressure gradients within the reacting sample

---

[*] Author for correspondence: rouquerol@up.univ-mrs.fr

1388–6150/$20.00

Akadémiai Kiadó, Budapest, Hungary
Springer, Dordrecht, The Netherlands

and thus results in a more reproducible experiment [19]. It gives generally better separation of intermediate stages in thermal decomposition. CRTA can also be used for kinetic studies of transformations [20].

The aim of this work is to highlight the importance of the residual pressure above the sample during the thermal decomposition of the gadolinium hydrogen phosphate trihydrate. Two residual pressures, $5\cdot10^{-3}$ and 5 mbar, were chosen and a number of intermediate samples were analysed by XRD, FTIR and SEM. These results permit thermal pathways for decomposition under each of the residual pressures to be proposed.

Experimental

Synthesis

The starting materials were 99% purity $GdCl_3\cdot6H_2O$ (Fluka) and 98% purity $Na_4P_2O_7\cdot10H_2O$ (Fluka). Crystals of $HGdP_2O_7\cdot3H_2O$ are obtained by mixing a sodium diphosphate solution with an acidic solution of gadolinium chloride and evaporation of the solvent at room temperature. The crystallization of $HGdP_2O_7\cdot3H_2O$ from the solution begins after a few days. The crystals are then isolated washed with distilled water and dried in air at room temperature [15].

Constant transformation rate thermal analysis

The experiments are carried out with 50 mg samples weighed into a fused silica cells which are placed into a refrigerated furnace constructed in house and operating in the 250–873 K temperature range.

Once the equilibrium temperature is reached, the pressure above the sample, measured by a Pirani gauge, is lowered, using vacuum pumping system from 1 bar to the desired value ($5\cdot10^{-3}$ mbar in our case). During the CRTA experiment where the reaction leads to the production of a vapour, the vapour pressure is measured by a Pirani gauge placed in proximity of the sample. The pressure signal produced by the Pirani gauge is sent to the furnace heating controller. The heating of the sample then takes place in such a way as to keep constant, at a preset value, the vapour pressure generated by the sample [17, 18].

The use of a diaphragm, placed between the Pirani gauge and the vacuum system, permits an increase of the residual pressure above the sample without changing the rate of water vapour elimination.

The coupling of the CRTA apparatus (in house) with a mass spectrometer (VG Quadrupoles) allows one to follow the nature of the gaseous phase produced by thermal decomposition [21]. In the case where the gas composition above the sample does not change, the vapour pressure is kept in a state of quasi-equilibrium: its rate of production during the dehydration is maintained constantly equal to its rate of elimination which is itself kept constant with time.

Under these conditions, the length of each dehydration step varies proportionally with the mass of water loss. The plot of temperature *vs.* time thus obtained by CRTA is analogue to a thermogravimetric curve. Under these controlled conditions of constant rate, the time is directly related to a given mass loss and thus direct comparisons between curves obtained via CRTA and conventional TG can be made.

X-ray powder diffraction

X-ray powder diffraction studies were carried out on a PHILIPS PW 3710 diffractometer using CuK_α radiation.

IR spectroscopy

The IR spectra were recorded in the 4000–400 cm^{-1} range, on a PerkinElmer FTIR 1000 spectrophotometer. The powder was finely ground and pressed into KBr pellets.

Results

Thermal behaviour under 5 mbar water vapour pressure

The CRTA curves of the trihydrated gadolinium diphosphate obtained under residual vapour pressure of 5 mbar are shown in Fig. 1. The temperature curve ‘I’ shows the sample temperature variation with

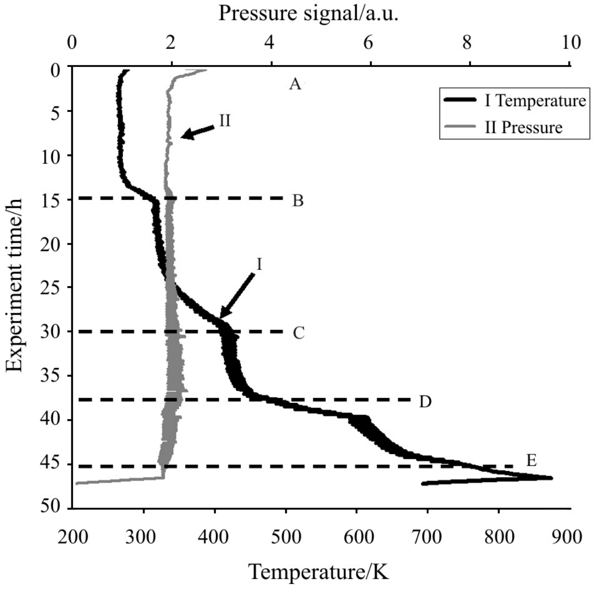

Fig. 1 CRTA curve of $HGdP_2O_7\cdot3H_2O$ under 5 mbar water vapour pressure

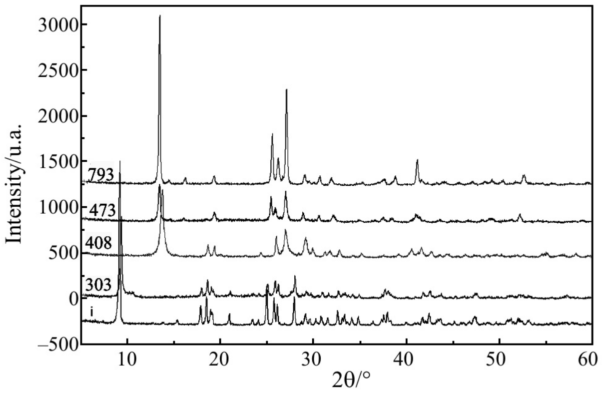

Fig. 2 X-ray diffraction patterns of $HGdP_2O_7·3H_2O$ (*i*) and of intermediate products obtained at different temperatures (K) under 5 mbar water vapour pressure

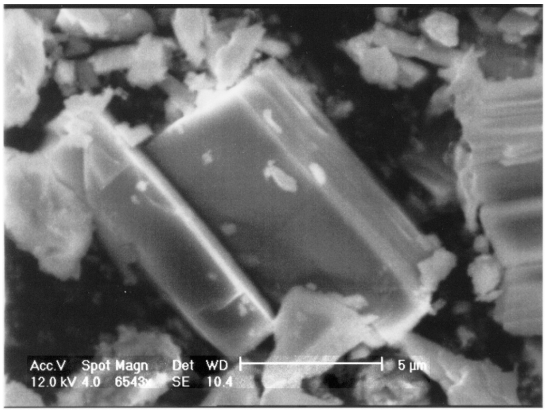

Fig. 4 SEM image of $HGdP_2O_7·3H_2O$ heated to 303 K by CRTA under 5 mbar water vapour pressure

time, controlled so as to keep constant the pressure (curve ‘II’). The variation in slope of the temperature curve, as well as the regulation changes that appear in the pressure curve allow the delimitation of four decomposition steps occurring respectively between 267–303 K (A–B), 303–408 K (B–C), 408–473 K (C–D), 473–793 K (D–E). The length ratio of steps (AB), (BC), (CD) and (DE) is 2 / 2 / 1 / 1 respectively.

The analysis of the final product, obtained at 793 K, by X-ray powder diffraction (Fig. 2) shows that the thermal decomposition leads to the anhydrous gadolinium diphosphate [10]. According to this result, the four decomposition steps, noted on the CRTA curves correspond to the complete dehydration of the trihydrated gadolinium diphosphate. Thus, the atmosphere surrounding the sample along thermal decomposition is formed only by the water vapour generated by the complex itself. Under these conditions the experiment is carried out not only under a constant residual water vapour pressure, but at a constant rate of dehydration [18]. The first two decomposition steps, having roughly the same length, can be attributed to the removal of the same quantity of water from the trihydrate. The remaining quantity of water is lost in equal amounts during the following two steps.

To characterise the products obtained at the end of each dehydration step, the CRTA experiment is restarted under identical conditions of rate and pressure; and the reaction is stopped at the temperatures determined from the initial curves (points B, C, D). The obtained intermediate products are immediately submitted to IR and X-ray powder diffraction studies.

According to the CRTA curve, the product isolated at 303 K would seem to be that of the dihydrate whereas the X-ray diffraction pattern (Fig. 2) would suggest the trihydrated salt. However, the XRD peaks are slightly shifted to larger angles. This result suggests that the removal of the first water molecules from the trihydrate, under the chosen conditions, takes place without any lattice transformation. This is confirmed by the IR spectroscopy (Fig. 3) where there is no change in peak positions. The only difference in the IR spectra obtained with the initial product and that obtained with the sample isolated at 303 K is the decrease in relative height of the bands due to water (around 3400 cm^{-1} and 1620 cm^{-1}). A comparison of

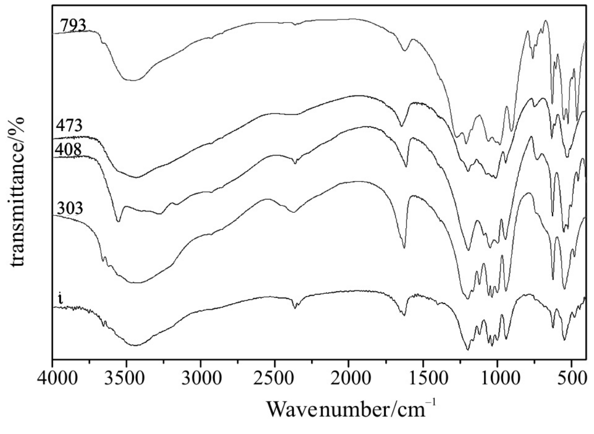

Fig. 3 IR spectra of $HGdP_2O_7·3H_2O$ (i) and of intermediate products obtained at different temperatures (K) by thermal decomposition under 5 mbar water vapour pressure

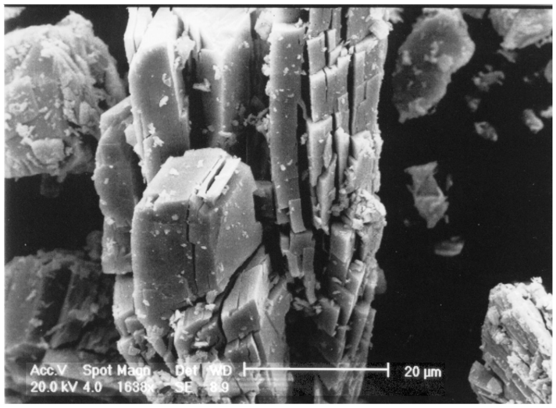

Fig. 5 SEM image of $HGdP_2O_7·3H_2O$ heated to 793 K by CRTA under 5 mbar water vapour pressure

the SEM image obtained for the sample treated to 303 K (Fig. 4) with the initial sample (not shown) suggests that the crystal morphology is preserved during CRTA treatment up to 303 K (Fig. 4). This confirms the fact that the loss of the initial water molecules during this first step has little or no effect on the lattice architecture. This is not the first time that such phenomenon has been observed during CRTA treatments. Indeed, the loss of the initial water molecules from $Ni(NO_3)_2{\cdot}6H_2O$ [22] and from gypsum [23] using CRTA, also occur with little or no change in the initial crystal architecture. This highlights the 'soft chemistry' nature that an SCTA treatment can provide.

The X-ray diffraction pattern of the hydrate prepared at 408 K (Fig. 2) is different from that of the initial product and can be attributed to the monohydrated gadolinium diphosphate. The corresponding IR spectrum (Fig. 3) is also different from that obtained for $HGdP_2O_7{\cdot}3H_2O$. The (POP) symmetric stretching vibration band, which was absent in the trihydrated salt spectrum, is observed at 750 cm^{-1} in the monohydrate spectrum. There is also a splitting of the water stretching band to three components between 3000 and 3500 cm^{-1}, which indicates the existence of different hydrogen bonding in the isolated diphosphate.

The X-ray pattern of the compound obtained at 473 K (Fig. 2), identified as the hemihydrate according to the CRTA results shows the existence of narrow peaks indicating the formation of a new crystallized product. This pattern is quite different from those of the trihydrate and monohydrate phosphates.

The X-ray pattern of the product isolated at 793 K (Fig. 2) is similar to that of the hemihydrated salt, however, it presents a non systematic displacement of peaks. This pattern is found to be similar to that given by Afonin [10] for $HLnP_2O_7$ (*Ln*=Dy, Er, Yb, and Y). This indicates that the final product is the anhydrous gadolinium diphosphate $HGdP_2O_7$ and that it is isostructural with $HLnP_2O_7$ (*Ln*=Dy, Er, Yb, and Y) compounds.

The IR spectrum of the product isolated at 793 K (Fig. 3) differs from the hemihydrate by the splitting of the νs(POP) vibration band to three components situated between 777 and 695 cm^{-1}.

The SEM image obtained for the final product (Fig. 5) shows large cracks on the surface indicating that the loss of the last water molecule degrades the crystal structure.

Thermal behaviour under $5{\cdot}10^{-3}$ mbar vapour pressure

The CRTA curve of $HGdP_2O_7{\cdot}3H_2O$, obtained under $5{\cdot}10^{-3}$ mbar vapour pressure, is shown in Fig. 6. This curve shows three decomposition steps: 250–423 K (A–C); 423–468 K (C–D) and 468–620 K (D–E). They have a length ratio of 2.8 / 1 / 1.

The final product obtained at 873 K is found to be the anhydrous gadolinium diphosphate. The three decomposition steps observed between 250 and 620 K can be initially attributed to the removal of the three crystallisation water molecules from the gadolinium hydrogen diphosphate.

Intermediate samples were obtained, by CRTA under $5{\cdot}10^{-3}$ mbar, corresponding to points B, C and D on Fig. 6. These were characterized by X-ray powder diffraction (Fig. 7) and IR spectroscopy (Fig. 8). The results were compared to those obtained in the case of CRTA under 5 mbar.

The X-ray diffraction pattern (Fig. 7) obtained with the intermediate obtained at 335 K (point B, Fig. 6) suggests the formation of a poorly crystallized

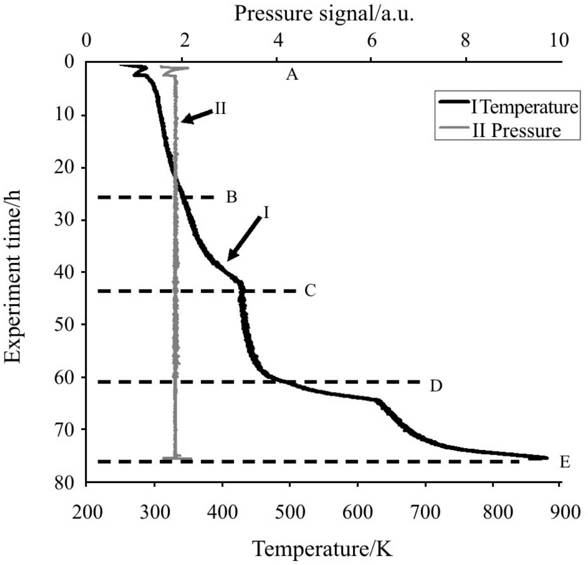

Fig. 6 CRTA curve of $HGdP_2O_7{\cdot}3H_2O$ under $5{\cdot}10^{-3}$ mbar water vapour pressure

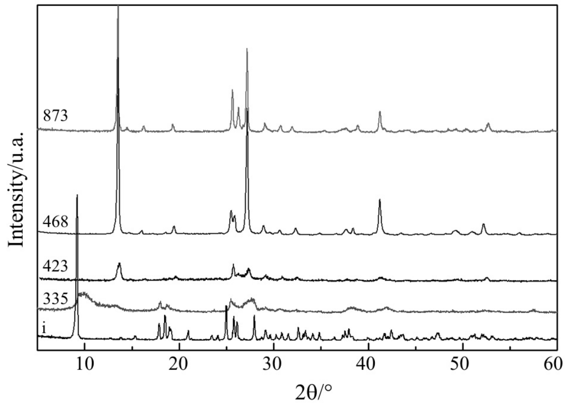

Fig. 7 X-ray diffraction patterns of $HGdP_2O_7{\cdot}3H_2O$ (i) and of intermediate products obtained at different temperatures (K) under $5{\cdot}10^{-3}$ mbar water vapour pressure

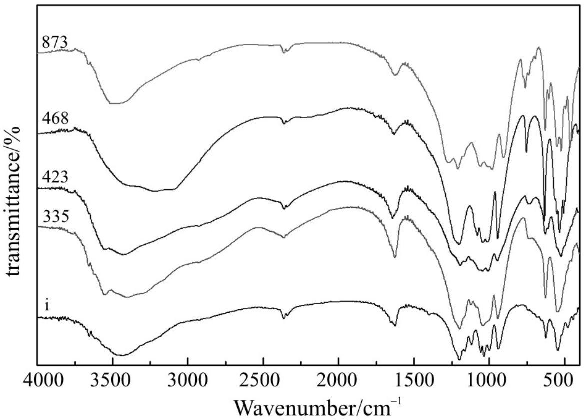

Fig. 8 IR spectra of $HGdP_2O_7.3H_2O$ (*i*) and of intermediate products obtained at different temperatures (K) under $5{\cdot}10^{-3}$ mbar water vapour pressure

phase. The X-ray diffraction pattern (Fig. 7) of the intermediate isolated at 423 K (point C, Fig. 6), again shows the formation of a poorly crystallized phase, the structure of which is different from that of the trihydrate. The corresponding IR spectrum (Fig. 8) shows broadened bands, however it is possible to note the existence of characteristic bands due to crystallization water (3500 and 1500 cm^{-1}) and diphosphate groups (1200 and 750 cm^{-1}).

For the product isolated at 468 K (point D) (Fig. 6), the X-ray diffractogram of the product isolated is identical to that of the hemihydrate isolated by CRTA under 5 mbar. This result is verified by IR spectroscopy (Fig. 8).

Discussion

Thermal behaviour at 5 mbar vapour pressure

The CRTA carried out under 5 mbar water vapour pressure suggests that the first decomposition step taking place between 267 and 303 K corresponds to the removal of one water mole from the trihydrate. X-ray powder diffraction and IR spectroscopic studies highlights that the first water loss occurs without any lattice transformation. To explain this result, it is necessary to consider the atomic arrangement of $HGdP_2O_7{\cdot}3H_2O$ [15].

A crystallographic study of the trihydrate shows that it crystallizes in the P_{-1} space group with two formula units per unit cell. Its structure is built by $HP_2O_7^{3-}$ anions which assemble themselves by pairs, interconnected by strong hydrogen bonds, and located around the inversion centre at (0, 0, 1/2) (Fig. 9). They generate a large channel parallel to the b axis, in which three pairs of crystallisation water molecules are located : W1, W2, W3 and their inversion centred symmetrical counterparts.

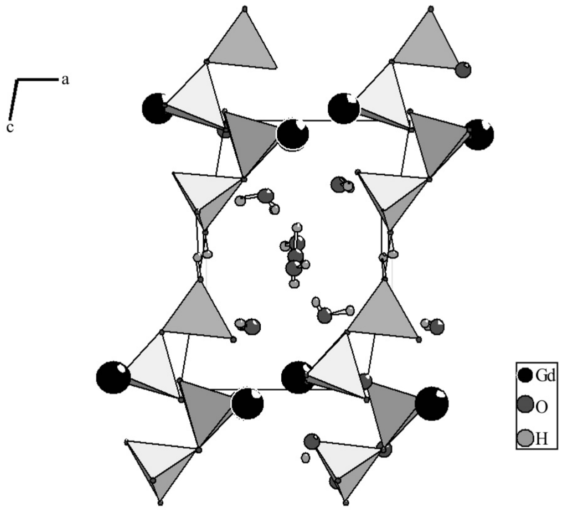

Fig. 9 Projection along b axis of the atomic arrangement in $HGdP_2O_7{\cdot}3H_2O$

The oxygen of the W3 water molecule is the only one having a high temperature factor; it is split in half occupied positions. The corresponding hydrogen atoms are not engaged in any hydrogen bonds with any other oxygen. These characteristics would seem to show that if the dehydration occurs very slowly under ‘soft chemistry-like’ conditions as induced by CRTA, the W3 water molecule and its symmetrical one can be removed from the $HGdP_2O_7{\cdot}3H_2O$ unit cell through the zeolitic-type channel without altering the initial crystalline structure. This can justify, under 5 mbar, the formation of a dihydrate during the first dehydration step having the same crystalline structure as the trihydrate.

As a topotactic transformation is assumed to be a solid phase chemical reaction which leads to a material with crystalline orientation related to the orientation of the initial product. Such a topotactic transformation of the trihydrated acidic gadolinium diphosphate to the dihydrate under 5 mbar water vapour pressure is proposed here.

The remaining four water molecules (W1, W2 and their symmetric ones) in the $[HGdP_2O_7{\cdot}3H_2O]_2$ unit cell belong to the coordination sphere of the gadolinium cation. The two pairs of molecules differ by the number of hydrogen bonds that they establish. The W2 water molecules are found to be engaged in one hydrogen bond through the H(22) hydrogen, with an external oxygen of the diphosphate group. Although the W1 molecules are engaged in two hydrogen bonds with two different external oxygens through H(11) and H(12). This suggests that the W2 water molecules are able to leave the crystalline network in the second dehydration step under 5 mbar between 303 and 408 K. During this step a reorganisation in the triclinic trihydrate structure takes place leading to the monohydrate structure.

The W1 water molecules remaining in the monohydrate structure are removed in two stages between 408 and 793 K leading to the structure of the anhydrous structure.

Thermal behaviour at $5\cdot10^{-3}$ mbar vapour pressure

The $HGdP_2O_7\cdot3H_2O$ thermolysis carried out under $5\cdot10^{-3}$ mbar shows the formation of the anhydrous compound at 620 K and the formation at 468 K of a hydrate having the same X-ray diffractogram as the hemihydrate isolated during CRTA under 5 mbar. These results suggest that the last dehydration step occurring between 468 and 620 K under $5\cdot10^{-3}$ mbar vapour pressure, can be attributed to the loss of one water mole from the $[HGdP_2O_7\cdot3H_2O]_2$ unit cell.

Since the second dehydration step occurring between 423 and 468 K, has the same length as the third one (468–620 K), it must also be attributed to the removal of a further water mole per unit cell.

Considering that the $[HGdP_2O_7\cdot3H_2O]_2$ unit cell contains six water molecules, the first dehydration step must be attributed to the loss of four water moles. This requires a step which is four times longer than the second or the third step. However, the CRTA results show that the first step is only 2.8 times longer than the two others. To explain this result it was necessary to take a closer look at the relationship between the residual pressure used in this study and the temperature of the start of the CRTA experiment. According to bibliographic data [24] the pressure of water vapour over ice at 250 K, which is the lower limit of temperature used in the CRTA experiment, is 0.8 mbar. That means that if the residual pressure decreases below 0.8 mbar at 250 K the equilibrium between ice and ice vapour is shifted towards the vapour.

As the W3 water molecules are weakly bound to the crystalline network, we can easily imagine that the dehydration of the gadolinium salt at 250 K starts as soon as the pressure reaches 0.8 mbar when applying the vacuum to the sample and before starting to heat. Indeed in this experiment we have gone down in pressure to $5\cdot10^{-3}$ mbar at 250 K. Thus we have lost some crystallization water before the start of the experiment. This can explain the shortness of the first dehydration step.

This phenomenon does not occur in the case of CRTA under 5 mbar water vapour pressure. Under such conditions, the dehydration can only begin from a temperature of 270 K which is above the starting temperature of the experiment.

Comparison with conventional thermogravimetric results

The CRTA results are different from those obtained by conventional thermogravimetry under an argon atmosphere at 5 K min^{-1}. This difference is most notable at low temperatures:

$$2[HGdP_2O_7,3H_2O]=2[HGdP_2O_7,1.5H_2O]+3H_2O(g)$$
345–423 K

$$2[HGdP_2O_7,1,5H_2O]=2[HGdP_2O_7,0.5H_2O]+2H_2O(g)$$
423–560 K

$$2[HGdP_2O_7,0.5H_2O]=2HGdP_2O_7+1H_2O(g)$$
638–773 K

Under such conditions it is possible to imagine that the water vapour generated by the salt is not completely eliminated by the argon flow because of the high rate of dehydration in a thermogravimetric experiment. Thus it would seem that in a traditional linear heating rate thermogravimetric experiment the thermolysis takes place under a poorly defined residual water vapour pressure which is intermediate between $5\cdot10^{-3}$ and 5 mbar.

Conclusion

This study highlights the influence of the residual water vapour pressure on the thermal decomposition of the gadolinium hydrogen diphosphate trihydrate. Under an experimental pressure of 5 mbar the transformations observed for $HGdP_2O_7\cdot3H_2O$ can be represented schematically by the following steps:

$$2[HGdP_2O_7,3H_2O]=2[HGdP_2O_7,2H_2O]+2H_2O$$
267–303 K

$$2[HGdP_2O_7,2H_2O]=2[HGdP_2O_7,H_2O]+2H_2O$$
303–408 K

$$2[HGdP_2O_7,H_2O]=2[HGdP_2O_7,0.5H_2O]+H_2O$$
408–473 K

$$2[HGdP_2O_7,0.5H_2O]=2HGdP_2O_7+H_2O$$
473–793 K

Whereas under a $5\cdot10^{-3}$ water vapour pressure the decomposition scheme is :

$$2[HGdP_2O_7,3H_2O]=2[HGdP_2O_7,2H_2O]+4H_2O$$
250–423 K

$$2[HGdP_2O_7,2H_2O]=2[HGdP_2O_7,H_2O]+H_2O$$
423–468 K

$$2[HGdP_2O_7,H_2O]=2[HGdP_2O_7]+H_2O$$
468–873 K

All intermediate hydrates isolated under the two residual pressures were characterized by IR spectroscopy and X-ray diffraction.

It would seem from these results that under a sufficiently low water vapour pressure, the crystallization water is eliminated in a continuous manner, presumably by diffusion in the zeolitic channels existing in the atomic arrangement of $HGdP_2O_7,3H_2O$. In this case the thermal treatment does not permit a crystalline rearrangement during the reaction. A progressive disorganisation of this latter structure and the passage by a quasi-amorphous state is observed.

On the other hand, under the higher water vapour pressure of 5 mbar, the crystallization water is eliminated with a more discontinuous way. Well marked stages are then observed more readily. This encourages the reorganization of the crystalline structure and leads to well crystallized intermediate products.

References

1 C. Brecher, J. Chem. Phys., 61 (1974) 2297.
2 H. G. Danielmeyer and H. P. Weber, I. E. E. J. Quantum Electronics, QE-8 (1972) 805.
3 H. Y. P. Hong and K. Dwight, Mat. Res. Bull., 9 (1974) 775.
4 G. Huber and H. G. Danielmeyer, J. Appl. Phys., 18 (1979) 77.
5 S. Colak and W. K. Zwicker, J. Appl. Phys., 54 (1983) 2156.
6 S. R. Chinn and H. Y. P. Hong, Appl. Phys. Lett., 26 (1975) 649.
7 K. Otsuka, S. Miyazawa, T. Yamada, H. Iwasa and J. Nakano, J. Appl. Phys., 48 (1977) 2099.
8 A. Akrim, D . Zambon and J. C. Cousseins, J. Alloys Compd., 99 (1994) 207.
9 A. Akrim, D . Zambon and J. C. Cousseins, J. Res. Bull., 33 (1998) 5975.
10 E. G. Afonin and N. I. Pechurova, Russ. J. Inorg. Chem., 35 (1990) 783.
11 S. Ben Moussa, I. Sobrados, J. E. Iglesias, M. Trabelsi-Ayadi and J. Sanz, J. Mater. Chem., 10 (2000) 1973.
12 F. Chehimi-Moumen, D. Ben Hassen-Chehimi, M. Ferid and M. Trabelsi-Ayadi, J. Therm. Anal. Cal., 65 (2001) 87.
13 F. Chehimi-Moumen, M. Ferid, D. Ben Hassen-Chehimi, and M. Trabelsi-Ayadi, Solid State Sci., 4 (2002) 979.
14 S. Ben Moussa, S. Ventemillias, A. Cabeza, E. Gutierrez-Pueba and J. Sanz, Solid State Chem., 177 (2004) 2129.
15 F. Chehimi-Moumen, D. Ben Hassen-Chehimi, M. Ferid and M. Trabelsi-Ayadi, Mater. Res. Bull., 36 (2001) 365.
16 F. Chehimi-Moumen, M. Ferid, D. Ben Hassen-Chehimi and M. Trabelsi-Ayadi, Mat. Res. Bull., 36 (2001) 2175.
17 J. Rouquerol, Thermochim. Acta, 144 (1983) 203.
18 'Sample Controlled Thermal Analysis : Origin, Goals, Multiple Forms, Applications and Future', (O. Toft Sorensen & J. Rouquerol Eds.), Kluwer Acad. Publishers, Dordrecht, 2003.
19 J. Rouquerol, J. Therm. Anal. Cal., 72 (2003) 1081.
20 J. M. Criado, J. Therm. Anal. Cal., 72 (2003) 1097.
21 J. Rouquerol, S. Bordère and F. Rouquerol, in 'Thermal Analysis in the Geosciences' (W. Smykatz-Kloss and S. St. J. Warne Eds.), Springer-Verlag, Berlin, (1991) pp. 134–150.
22 P. L. Lewellyn, V. Chevrot, J. Ragaï, O. Cerclier, J. Estienne and F. Rouquerol, Solid State Ionics, 101 (1997) 1293.
23 E. Badens, P. L. Lewellyn, F. Rouquerol, S. Vessler and R. Boistelle, J. Sol. State Chem., 139 (1998) 37.
24 CRC Handbook of Chemistry and Physics, (R. L. Lide Ed.) 75th Edn. 1994.

DOI: 10.1007/s10973-005-6930-2